Reciprocity-Based Simulation Methodology to Estimate the Power Distribution Received by Electro-Magnetic Energy Harvesters

Dimitar Nikolov Nikolov[1], Bart Gerard Boesman[2], Filip Vanhee[2], Emil Dimitrov Manolov[3], Marin Hristov Hristov[1], Renaat De Craemer[2], Davy Pissoort[2]

[1] Department of Microelectronics, Technical University of Sofia, 8 Kliment Ohridski Blvd., 1000 Sofia, Bulgaria email: {d.nikolov, mhistov}@ecad.tu-sofia.bg
[2] Reliability in Mechatronics and ICT Research Group, KU Leuven-Kulab, Zeedijk 101, Ostend B-8400, Belgium email: {bart.boesman, filip.vanhee, renaat.decraemer, davy.pissoort} @kuleuven.be
[3] Department of Electronics and Electronics Technologies, Technical University - Sofia, 8 Kliment Ohridski blvd., 1000 Sofia, Bulgaria email: edm@tu-sofia.bg

Abstract

The capability to efficiently harvest power from ambient energy sources is a crucial element for the development of low-maintenance wireless sensor networks. Available energy levels that can be harvested from ambient electromagnetic (EM) sources are rather low (0,1µW/cm^2). Insufficient information about the available EM energy under different working conditions results in poor design decisions, leading to a sub-optimal system design. In this paper, a novel and efficient simulation methodology is developed which predicts the statistical distribution of the power harvested by an antenna when immersed in a given (statistical) EM environment. The methodology is used to quantify the impact of the antenna's orientation, location, exact geometry, etc. on the quantity of the harvested energy. The methodology is successfully applied to a realistic energy harvesting antenna in different EM environments (indoor, outdoor,…)

1. Introduction

Nowadays, wireless sensor nodes (WSNs) are frequently used in data acquisition networks [1] and this within a wide variety of applications, such as e.g. infrastructure, transportation, health, industrial machinery monitoring, etc. Although most of the currently commercially exploited WSNs still operate on batteries [2], there is a continuous search for new green and renewable energy sources that allow the development of low-maintenance, perpetually running WSNs without the need for batteries or wires. The concept of energy harvesting is crucial to achieve this goal. The name “energy harvesting” refers to a set of technologies which enable to extract, convert and store energy from environmental sources. Energy can be harvested from different types of environmental sources [3], such as electromagnetic fields [4], vibrations [5], solar power [6], heat [7], wind[8], etc. The aim of energy harvesting is to allow the implementation of long-life and low maintenance power-autonomous electronic devices.

A typical block diagram of an autonomous WSN powered by energy harvesting is presented in Fig. 1 (taken from [9]). The sensor node consists of one or more sensors, an ultra-low power microcontroller, a low-power transceiver and an energy harvesting device. The energy harvesting device extracts energy from the environment and transforms it to electrical energy used to power the whole sensor node.

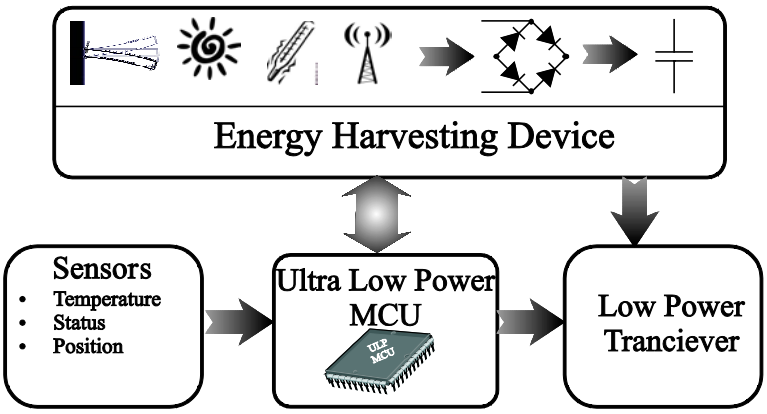

Fig. 1 Block diagram of autonomous sensor for wireless network.

The sensors monitor parameters of the examined object or its environment and transfer their readings to the ultra-low power microcontroller. The microcontroller processes the data and delivers them to the low-power transceiver which makes the connection to the central node or to other sibling nodes in the network. The energy required for autonomous operation of the WSN equals the sum of the energy needed for the operation of the micro-controller, transceiver and sensor. Making sure that sufficient power for uninterruptible node operation will be present during the whole foreseen lifetime of the WSN raises important challenges related to the prediction of the available energy under different circumstances.

In battery-powered devices, the logic way to extend the operational lifetime is to minimize the device's energy consumption. Reducing consumption in wireless sensor nodes is often realised by employing power modes e.g. off, stand-by, deep-sleep, decreasing power supply voltages, efficient signal processing [10] and minimizing the data transmission energy [11]. As a battery's capacity is the amount of electric charge it can deliver at the rated voltage, the energy budget for battery-powered devices can be easily predicted. In contrast, using energy harvesting to power a device leads to problems related to the uncertainty about the accessible amount of energy. In general, insufficient information about the available energy results in poor design decisions [12], leading to a sub-optimal component. Under- or over - sizing components in the system, e.g. a supercapacitor or re-chargeable battery, causes overpricing or a reduced lifetime expectance [13]. Furthermore, failing to predict the amount of energy presence leads to non-optimal performance [14] due to the incapability of

planning the energy spending up-front. Hence, quantitative analysis of the available energy is crucial at the design stage in order to achieve an optimal design.

So far, algorithms for predicting the available energy have mostly been studied for harvesting solar power [12–15]. Based on these algorithms, improved working principles for solar energy harvesting devices have been proposed. For example, Kansal et al. proposed in [12] a prediction model based on Exponentially Weighted Moving-Average (EWMA) filter. The output from this prediction model is used to calculate a novel dynamic duty cycle algorithm which is significant improvement on naïve approach of 50% duty–cycling. Later on, Cammarano et al. presented in [13] a framework able to predict available solar and wind energy based on past-days observations. Their prediction model improves on the EWMA with more than 60 % and, moreover, relies only on data gathered from the WSN. Unfortunately, little or no prediction models are available for electromagnetic environmental energy sources.

Energy harvesting based on electromagnetic fields falls into two subcategories, namely near -field [16-17], and far-field [18-19]. In the near-field case, Kurs et al. [16] used self-resonant coils in a strongly coupled regime to transfer power via magnetic resonances. They reported successful transfer with ~40% efficiency over distances in excess of 2 meters. In a study which set out to realise reliable wireless power transfer for biomedical implants, Tucker et al. [20] presented 91% efficiency at power transfer over a 2 cm distance between transmitter and receiver. In the far-field case [18], the distance between the source of the electromagnetic energy and the receiving antenna is many wavelengths. Energy can be taken from ambient sources e.g. Wi-Fi, TV and radio broadcasting stations or dedicated transmitters [21]. Ambient electromagnetic sources have an energy density of about 0,3 $\mu W/cm^2$[22] while scavenged power density is typically 0,1$\mu W/cm^2$ [19]. Harvesters can be located in a wide variety of electromagnetic environments e.g. indoor, outdoor, with or without line of sight, etc. Different environments lead to diverse fading situations caused by the different propagation media.

The architecture of a device that converts incident electromagnetic energy to usable direct current (dc) power consists of antenna, impedance matching network, rectifier, energy reservoir and load. The antenna converts the incident RF power to AC currents and voltages, the matching circuit reduces reflection losses and increases the output voltage from antenna. The matching circuit output voltage is then rectified and stored in the energy reservoir. A recent study of Piñuela et. al. [4] investigated RF energy harvesting in urban and in semi-urban environments, and reported RF to DC efficiency of 40%. Sakamoto et al.[23] reported an array of series and parallel connected devices able to operate at 5.8-GHz with 38% RF-DC efficiency. Hagerty et al.[24] presented a broadband device harvesting RF energy between 2-18 GHz. In [19] powering an off-the shelf

temperature and humidity meter with energy harvested from wireless routers in an office environment was demonstrated. The DC power depends on the available RF power and since the rectifier consists of diodes which are non-linear devices, the input impedance depends on the input power. Nintanavongsa et al.[25] presented a dual-stage harvesting device, tackling the non-linear input impedance problem and operating at 915 MHz. Hence, a thorough understanding of the antenna output power is essential for the development process. To the best of our knowledge no solution has been provided to take into consideration the statistical nature of the electromagnetic environment together with the exact antenna's geometry and mounting.

To date various methods have been developed and introduced to characterize antenna coupling performance i.e. exact and asymptotic methods or combination of both referred as hybrid methods. Numerical methods e.g. finite-elements (FEM), Method of Moments (MoM) and finite-difference time-domain (FDTD) are effective, and work very well for models which have dimensions up to several wavelengths. When it comes to the study of the entire domain of propagation, these numerical methods require excessive computational resources both in terms of calculation and memory [26]. High-frequency asymptotic methods e.g. Geometrical Theory of Diffraction (GTD), which was developed by Keller[27] are used when dimension of the emitting objects are electromagnetically large. Hybrid coupling methods combine exact and asymptotic techniques and are able to handle electromagnetically large geometries, by accurately simulating antenna fields with exact methods and effectively consider the propagation environment effects with asymptotic or exact methods [28]. The current-based analysis is appropriate for handling complex geometries and it accurately represents the antenna properties in close proximity of near-by large objects. In contrast the field-based analysis is valuable at simulating canonical geometries. Mainly hybrid methods are split into two categories, current-based and field-based analysis [29]. In order to calculate power received by antenna, with abovementioned methods, the statistical properties of incident electromagnetic field are needed. However, so far, there has been little discussion about predicting the amount of the power output, which will be harvested from electromagnetic fields by an antenna.

In this paper, a novel and efficient methodology is proposed which enables to predict the statistical distribution of the power harvested by an antenna from a given electromagnetic environment allowing a designer to compare different options and make important decisions already at early design stages. At the heart of the methodology is the antenna-reciprocity based algorithm proposed in [30] for predicting the coupling of plane waves to cables. In this paper, the algorithm of [22] is applied to the coupling of EM waves to energy harvesting antennas and combined with the statistical description of typical electromagnetic environments [31]. The

algorithm is efficient as it requires only one full-wave simulation of the energy harvesting antenna as radiating device. Once the far-field radiation pattern and the antenna's input impedance are known, the statistical distribution of the received amount of power in whatever electromagnetic environment can be obtained. Therefore, the receiving antenna is described by its equivalent circuit, while the electromagnetic environment is modelled as a superposition of pseudo-random plane-waves which are chosen according to the statistical description of that environment. The proposed methodology gives the opportunity to quantify the impact of the antenna's orientation, location, exact geometry, etc. on the quantity of harvested energy.

The remainder of this paper is organized as follows. Section 2 briefly repeats the reciprocity-based algorithm to calculate the power received by an antenna when illuminated by a single plane wave. Section 3 gives an overview of the statistical representation of typical electromagnetic environments and explains how these can be modeled by means of pseudo-random plane waves. In Section 4, the versatility and efficiency of the algorithm is shown by applying it to the simulation of a typical antenna harvesting antenna in different environments and positions. Finally, the main conclusions of this work are summarized in Section 5.

2. Calculating the power received by an antenna based on reciprocity

This section summarizes the theoretical basis of the reciprocity–based algorithm proposed in [30] to calculate the power received by an antenna when illuminated by a single plane wave. The antenna reciprocity theorem states that the behaviour of a receiving antenna ('receive mode') is completely known once it has been characterized as radiating device [32] ('transmit mode'). Due to the reciprocity, the antenna's input impedance is

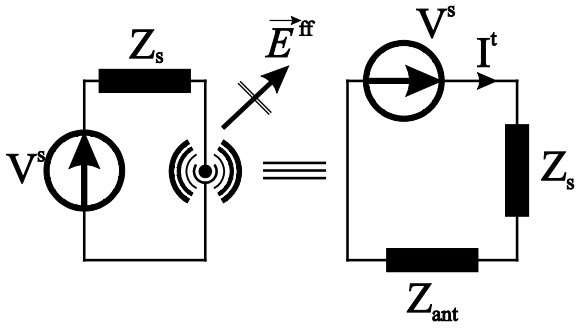

Fig. 2a. Equivalent circuit transmitting antenna simulation set-up.

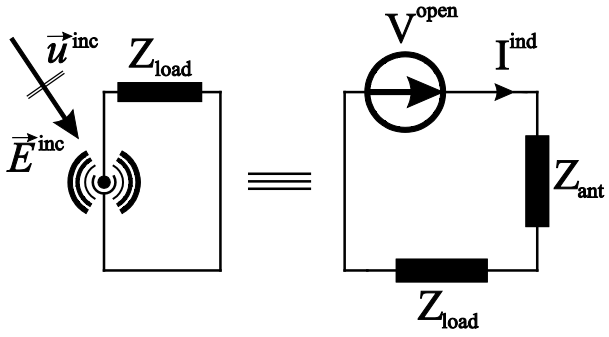

Fig. 2b. Equivalent circuit receiving antenna simulation set-up.

the same in receive and transmit mode. Further, knowledge of the far-field radiation pattern in transmit mode allows to transform whatever incoming plane wave into an equivalent voltage (or current) source in receive mode.

The different steps in the reciprocity-based technique are as follows. First, a full-wave simulation of the antenna as radiating device is performed. For a simulation set-up where the antenna with impedance Z_{ant} is fed by voltage source V_s with impedance Z_s, the equivalent antenna circuit in transmit mode is shown in Fig. 2a.. Based on this simulation the antenna's input impedance Z_{ant} as well as its far-field radiation pattern $\vec{E}^{\mathrm{ff}}$ are obtained with one full-wave simulation.

Second, the antenna's equivalent circuit in receive mode (see Fig. 2b) when illuminated by a given plane wave is determined. The antenna's input impedance is exactly the same as in transmit mode. If the incoming plane wave $\vec{E}^{\mathrm{inc}}$, is falling in from the direction $\vec{u}^{\mathrm{inc}}$ which is characterized by the angles θ and φ

(see Fig. 3), the equivalent voltage source is given by

$$V^{open}(\theta,\varphi,\psi) = -\frac{2j\lambda}{\eta}\frac{\left\|\vec{E}^{inc}\right\|\left(\vec{E}_{\theta}^{\mathrm{ff}}\cos(\psi)+\vec{E}_{\varphi,}^{\mathrm{ff}}\cos(\psi)\right)}{I^{\mathrm{t}}}, \tag{1}$$

Here, the polarization angle ψ is defined as the angle between the θ-axis and the incident plane wave's electric field (Fig. 3). Further, $\lambda = \frac{c}{f}$ is the free-space wavelength and $\eta = 120\pi$ is the free space impedance. Finally, I^{t} (Fig. 2a) is the current flowing into the antenna in transmit mode and is used to correctly normalize the far-field

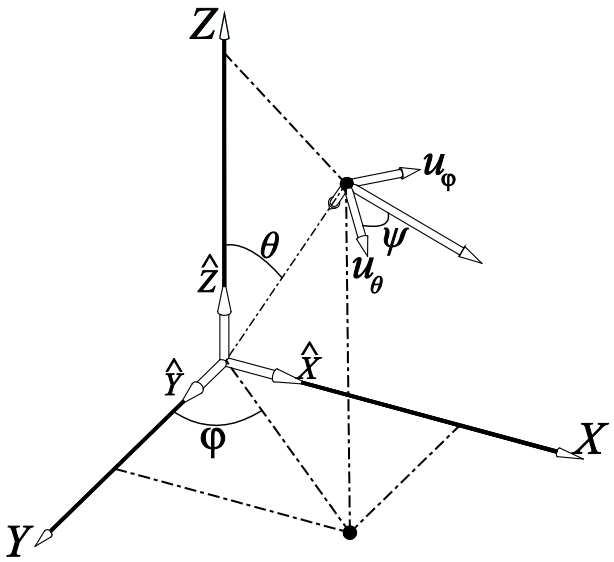

Fig. 3. Incident wave coordinate system definition.

pattern.

From the equivalent circuit in receive mode, the induced current I^{ind} can be easily obtained as

$$I^{\text{ind}} = \frac{V^{\text{open}}}{\text{Z}_{\text{ant}} + \text{Z}_{\text{load}}}, \tag{2}$$

The maximum power is received when the load is matched at the antenna's input impedance $\text{Z}_{\text{ant}} = \text{Z}_{\text{load}}^{*}$. Under this condition, and if $\Re[Z_{ant}] = \Re[Z_{load}] = \Re[Z_0]$, the expression for the received power simplifies to

$$P_{max}^{ind} = \frac{(|V^{open}|)^2}{4\Re[Z_0]}, \tag{3}$$

where $\Re[\text{Z}_{\text{ant}}]$ and $\Re[Z_{load}]$ are the real parts of the antenna's input impedance and the load, respectively.

3. Angular power density distributions in different propagation environments

In [33], Taga proposed a model to statistically describe the propagation properties of incoming electromagnetic waves in different environments. The statistical properties of the fields incident on an antenna are expressed as angular power density functions $Pr(\theta)$ and $Pr(\varphi)$ in elevation and azimuth respectively. In [33], these are assumed to be Gaussian in elevation (θ) and uniform in azimuth (φ). However, Taga conducted only 4 measurements to examine angular density functions of incident waves, which later turned out to be an insufficient number to provide statistically meaningful results. In a more comprehensive study [31], Diallo et al. proposed Laplacian and Elliptical distributions in elevation to describe indoor and outdoor propagation environments. This paper uses statistical distributions for different electromagnetic environments, proposed in aforementioned study [22]. These are summarized in Table 1.

In Table 1, m and σ mean polar angle for the incoming plane waves and the standard deviation, respectively. As indicated in Table 1, care has to be taken when implementing a uniform distribution for the elevation. Simply taking a uniform distribution of the angle θ over [0, π] would result in incoming angles that are "bunched" near the poles [35]. In order to get a real uniform distribution in which no direction-of-arrival gets any privilege, θ must be chosen such that $\cos(\theta)$ is uniformly distributed in [0, 1].

The above statistical distributions are combined with the reciprocity-based algorithm of Section II by representing them as the superposition of a finite, but large number (further denoted by *N*) of incident plane waves whose incoming directions, polarization, phase,… are randomly chosen according to the given statistical

Table 1 Statistical distributions representing different propagation environments.

	Elevation	Azimuth	Indoor	Outdoor
Uniform	$Pr(\theta) = \frac{1}{2}\sin\theta$	$Pr(\varphi) = \frac{1}{2\pi}$		
Gaussian Uniform	$Pr(\theta) = A_\theta \exp\left[-\frac{\{\theta - [(\pi/2) - m]\}^2}{2\sigma^2}\right]$	$Pr(\varphi) = \frac{1}{2\pi}$	$m = 10^\circ$ $\sigma = 15^\circ$ $XPR = 5$ dB	$m = 20^\circ$ $\sigma = 30^\circ$ $XPR = 1$ dB
Laplacian Uniform	$Pr(\theta) = A_\theta \exp\left[-\frac{\sqrt{2}\lvert\theta - [(\pi/2) - m]\rvert^2}{2\sigma}\right]$	$Pr(\varphi) = \frac{1}{2\pi}$	$m = 10^\circ$ $\sigma = 15^\circ$ $XPR = 5$ dB	$m = 20^\circ$ $\sigma = 30^\circ$ $XPR = 1$ dB

distributions. This is repeated a large number of times (further denoted by *M*) in a Monte-Carlo (MC) simulation to find the statistical properties of the induced current, power,… This representation is a direct extension of what is known as the plane-wave integral representation technique [36] which is used to numerically describe the fields within a reverberation chamber for e.g. the coupling to devices, cables,…[34].

In every step, the MC simulator generates pseudo random samples for the following variables: direction-of-arrival (DoA) angels (θ and φ), phase angle β and polarization angle ψ of the incoming plane waves. For every sample the induced voltage and/or current is determined as described in Section 2. The induced quantities are summed up for all *N* samples after which the maximally (or maximum) received power is calculated. This is repeated *M* times in order to get the statistical distribution of the received power.

The phase angle is uniformly distributed in [0, π]. The distribution of the polarization angle is somewhat more complicated. The cross polarization ratio XPR [24] is a parameter which is not known or needed for the description of the statistical fields in a reverberation chamber. The XPR is the ratio of the mean incident power of vertically(i.e. $\oiint_{4\pi}|E_\vartheta|^2 d\Omega$)) and horizontally polarized incoming plane waves(i.e. $\oiint_{4\pi}|E_\varphi|^2 d\Omega$):

$$\text{XPR} = \frac{\oiint_{4\pi}|E_\vartheta|^2 d\Omega}{\oiint_{4\pi}|E_\varphi|^2 d\Omega}, \tag{4}$$

An XPR different from 1 (i.e. 0dB) means that on average over the whole sphere more power is falling in from one of the polarizations. This means that in these cases there is a preferred polarization. In the modelling, this can be taken into account by introducing an appropriate statistical distribution for the polarization angle ψ. When the XPR=0dB, the statistical distribution for ψ is uniform in the range between $-\frac{\pi}{2} \leq \psi \leq \frac{\pi}{2}$. For XPR $\neq$ 0dB, the statistical distribution for ψ is taken as a truncated Gaussian in the range between $-\frac{\pi}{2} \leq \psi \leq \frac{\pi}{2}$, whose mean value and standard deviation are chosen such that eq. (4) is fulfilled.

The distribution of the polarization angle ψ is given in Table 2 for a few typical cases.

Table 2 Distribution of polarization in accordance to a given XPR.

XPR	Range	Type distribution	Mean	Standard deviation
5 [dB]	$-\frac{\pi}{2} \leq \psi \leq \frac{\pi}{2}$	Truncated Gaussian	0	$\frac{\pi}{5.4}$
1 [dB]	$-\frac{\pi}{2} \leq \psi \leq \frac{\pi}{2}$	Truncated Gaussian	0	$\frac{\pi}{2.2}$
0 [dB]	$-\frac{\pi}{2} \leq \psi \leq \frac{\pi}{2}$	Uniform	–	–
-1 [dB]	$-\frac{\pi}{2} \leq \psi \leq \frac{\pi}{2}$	Bimodal Truncated Gaussian	$-\frac{\pi}{2}$ & $\frac{\pi}{2}$	$\frac{\pi}{2.2}$
-5 [dB]	$-\frac{\pi}{2} \leq \psi \leq \frac{\pi}{2}$	Bimodal Truncated Gaussian	$-\frac{\pi}{2}$ & $\frac{\pi}{2}$	$\frac{\pi}{5.4}$

The amplitude of each incoming plane wave is related to the chosen expected value E_0 of the total incoming electric field and is determined as follows. The total power P [34] of a single incoming plane wave is given by

$$P \sim N E_N^2, \tag{5}$$

where E_N is the amplitude of a single plane wave. In order to obtain a given value for the total incoming field (i.e. the superposition of all incoming plane waves), E_N needs to be normalized with respect to N as follows

$$E_N = \frac{E_0}{\sqrt{N}} \tag{6}$$

Density function for different XPR values listed in Table 2 are shown in Fig. 4

In the following examples, E_0 is set to 1 V/m.. The resulting total electric field has a good agreement with the measured data shown in [37].

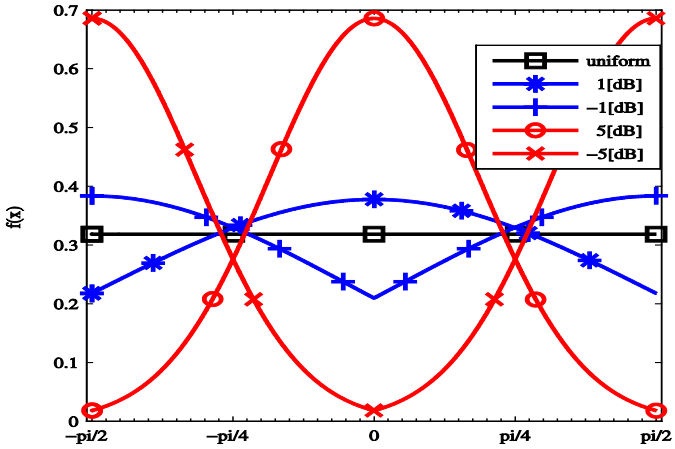

Fig. 4 Density function of the polarization angle ψ

4. Examples

In order to illustrate the effectiveness and applicability of the proposed algorithm, it is applied in this section to the coupling between ambient electromagnetic sources and a typical energy harvesting antenna.

In the examples that follow, the harvesting antenna is the one provided by PowerCast [21] for their evaluation board. All full-wave simulations are performed with the FDTD solver of EMPro from Agilent Technologies [38]. However, the proposed methodology can be applied to all EM simulation techniques that allow obtaining the antenna's input impedance and far-field pattern.

The energy harvesting system consists of two main parts: the antenna and supplementary printed circuit board (PCB). Here, the supplementary PCB has a double sided layout. One side is a full ground plane. On the

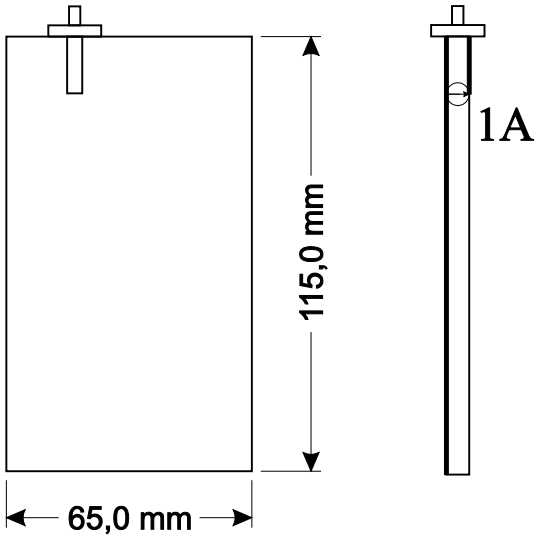

Fig. 5. Suplementary PCB simulation ser-up

other side, a 50 Ω microstrip line is connected to the antenna. In order to obtain the far-field radiation pattern, the configuration depicted in Fig. 2a. is considered: a 50 Ω voltage source excites the antenna at the microstrip as Fig. 5 shows .

As a first application, the impact of the antenna location i.e., indoor or outdoor, is studied. As a second application, the impact of the positioning of the harvesting antenna along the PCB is examined. The received power cumulative distribution functions (CDF) are obtained after conducting a MC simulation with N – 100

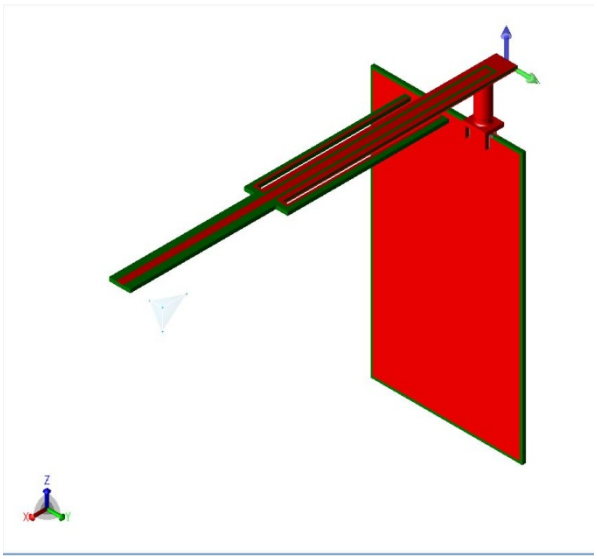

a) Position 1.

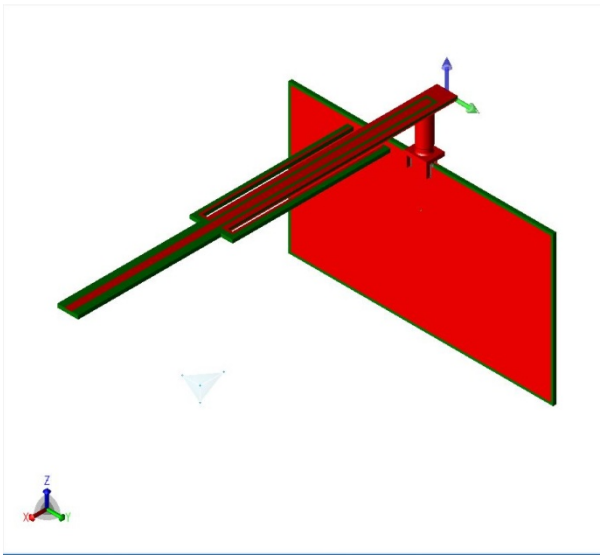

b) Position 2.

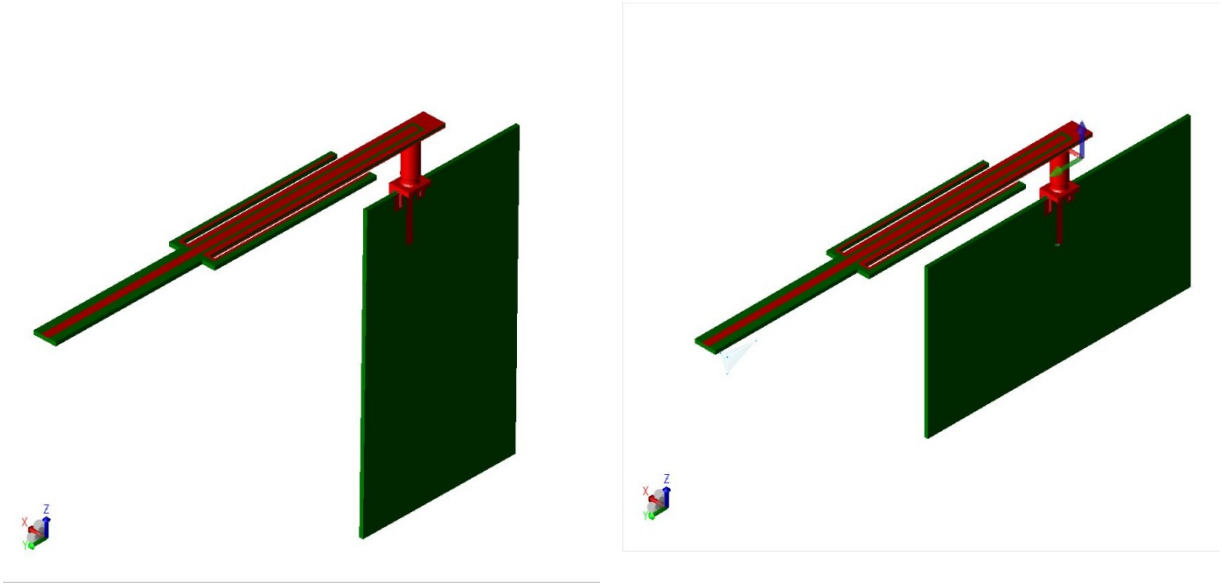

c) Position 3. d) Position 4.

Fig. 6 Antenna and PCB relative positions

and M - 50 x10^3 and for single frequency point 915 MHz. Four different relative positions between PCB and antenna are considered and shown in Fig. 6.

4.1 Statistical distribution of the total incoming field

This section demonstrates the total incoming field created with MC algorithm that uses superposition of the pseudo-random waves. Plane wave properties are chosen according to the statistical description of the environment, as was described in Section 3. Fig. 7 shows the histogram of total incoming field strength for the aforementioned MC simulation configuration (N – 100 and M - 50 x10^3) and is used for all the examples below. The data is obtained after conducting the MC simulation and keeping track for all the generated pseudo random samples. In Chapter 7 [37] and in [39] Hill, performed measurements of a electric field magnitude within the reverberation chambers and the statistical distribution of measured data shows good agreement with our MC generated field.

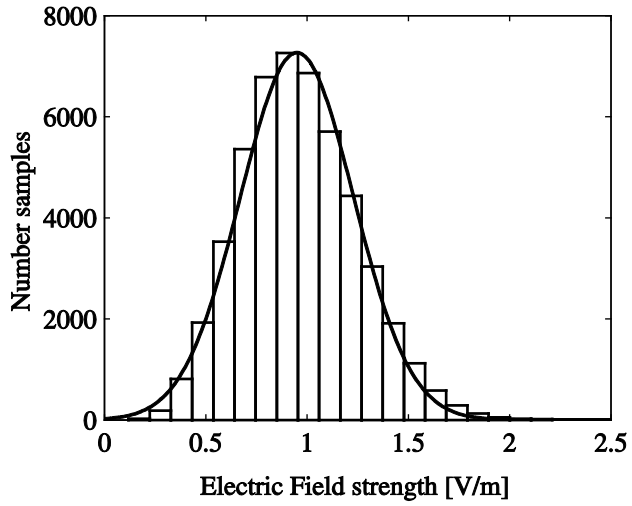

Fig. 7 Histogram of electric field strength

4.2 Influence of the EM environment on the received power

As a first application, a comparison is drawn between the CDFs of the (maximal) power received by the (matched) antenna for indoor and outdoor environment, as well as the full uniform distribution. The indoor and outdoor environments are represented by Gaussian statistical distributions, uniform distribution is used as a reference and the distributions are described in Table 1. The CDFs are presented in Fig. 8.

The CDFs shown in Fig. 8 describe the probability that the power received by the antenna will have a value less than or equal to the one presented on the *x*-axis. With these CDFs, a designer gains knowledge about

Fig 8 Comparision between received power in different propagation environments.

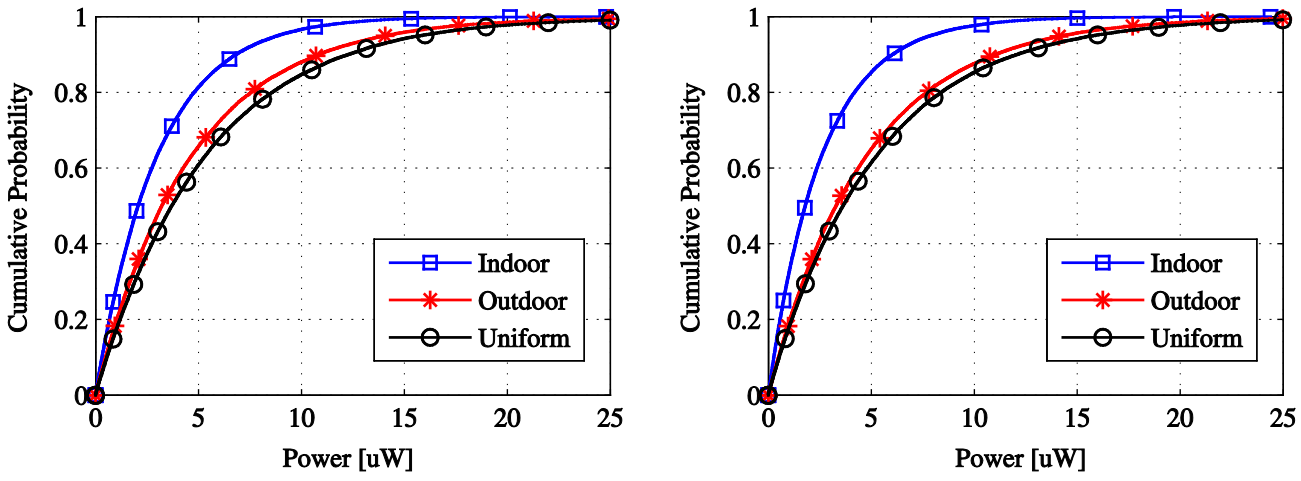

Fig. 8a. CDFs in position 1.

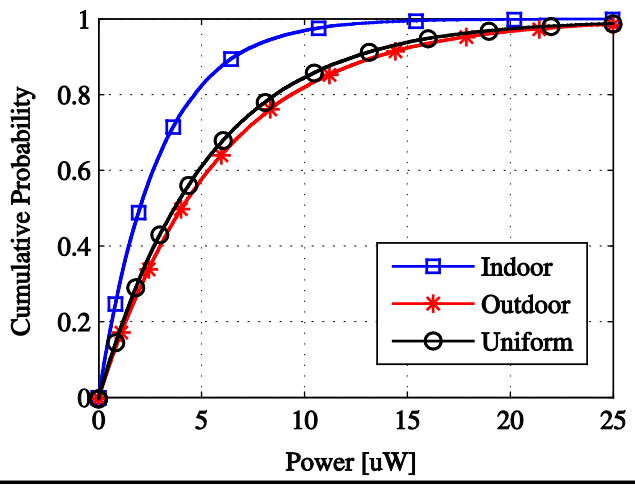

Fig. 8b. CDFs in position 2.

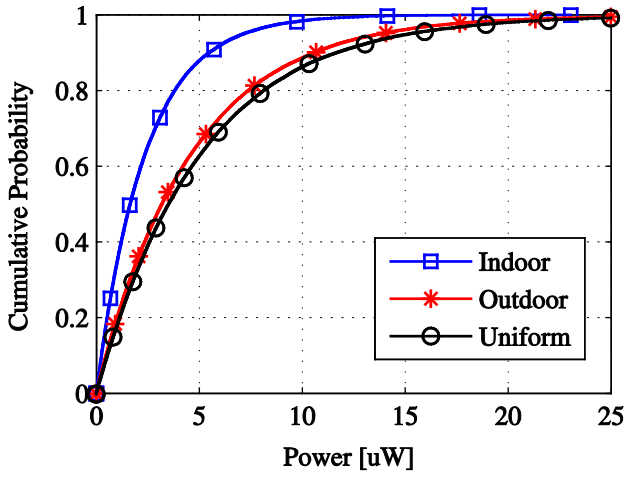

Fig. 8c. CDFs in position 3.

Fig. 8d. CDFs in position 4.

the statistical distribution of the received power for the different electromagnetic environments. For example, Fig 8c shows that received power in an outdoor environment is more than the power received in the uniform case.

4.3 Influence of the relative position of the antenna along the PCB on the received power

As a second application, a comparison between the CDFs is given for the four different antenna-PCB positions shown in Fig. 6. These CDFs are shown in Fig. 9. Each graph corresponds with one of the positions

Fig 9 Comparision between received power in different antenna positions.

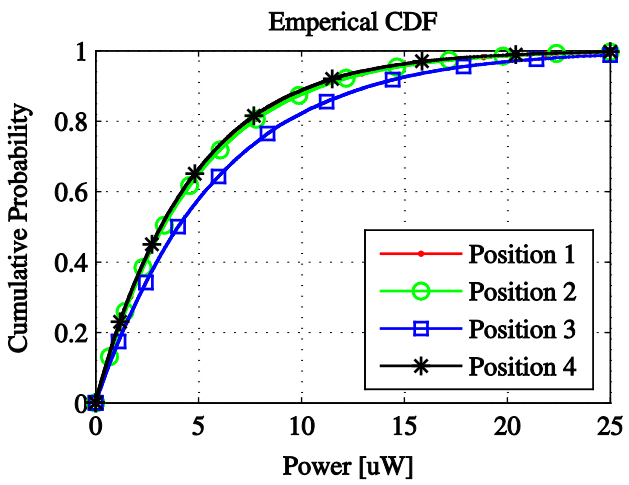

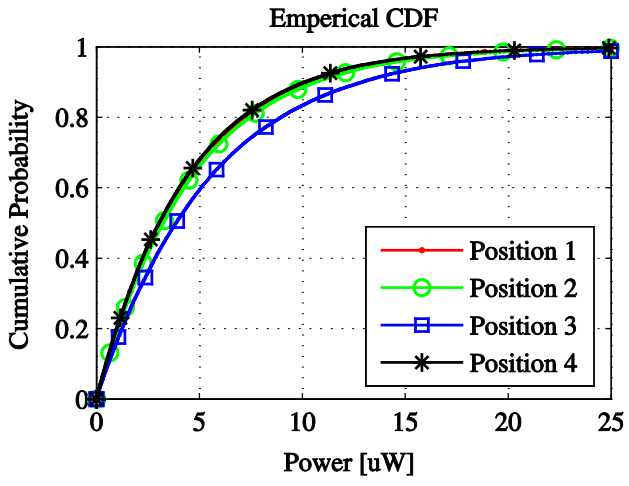

Fig. 9a. CDFs outdoor gaussian

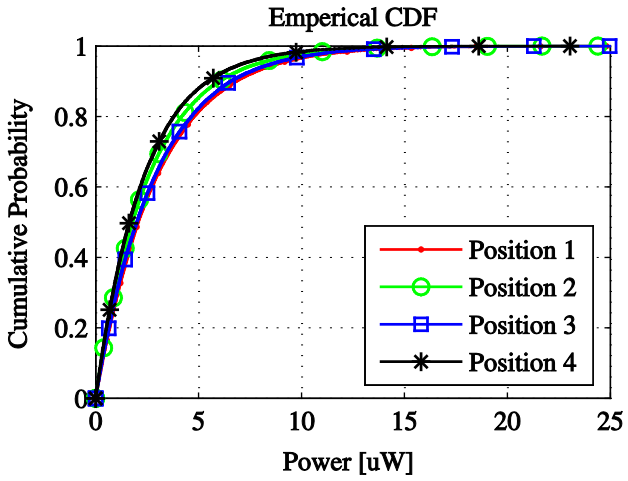

Fig. 9b. CDFs outdoor laplacian

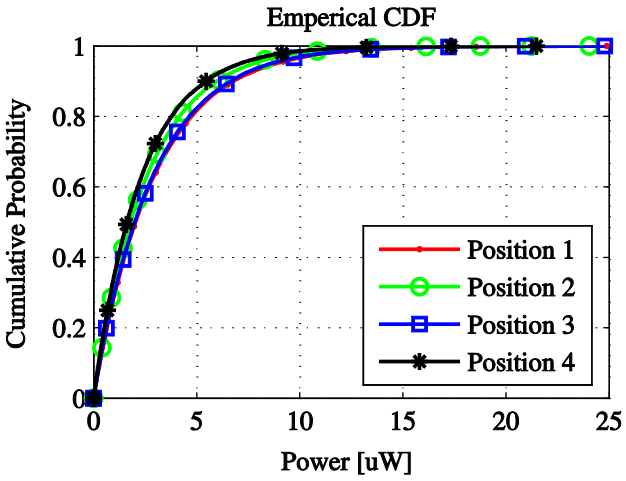

Fig. 9c. CDFs indoor gaussian

Fig. 9d. CDFs indoor laplacian

shown in Fig. 6. These CDFs are shown in Fig. 9.. Each graph corresponds with one of the EM environments given in Table 1 and compare different antenna positions.

The results shown in Fig. 9 indicate that the relative position of the harvester PCB influences the amount of received power. For example, in position 3 the amount of received power is higher than the other positions. The amount of received power is in the range of ten microwatts, caused by performing simulation only for a single frequency point. RF energy harvesters however are designed to work in specific frequency range.

5. Conclusion

An efficient reciprocity-based algorithm that allows to predict the available energy at an energy harvesting antenna's port was presented. Such an algorithm plays an important part in designing long-life and low maintenance power-autonomous electronic devices (especially WSNs). The proposed methodology takes into account all details of the antenna's geometry, its mounting onto the PCB as well as the EM environment in which the antenna is located. The algorithm is efficient as it only requires one full-wave simulation of the antenna as radiating device. Thanks to reciprocity, the distribution of the received power can be easily calculated without new full-wave simulations. The statistical nature of the EM environment is taken into account by representing it as a superposition of randomly chosen incoming plane waves according to the known statistical distributions of the environment. By means of a MC simulation, the statistical distribution of the received power is obtained.

The methodology was applied to a realistic energy harvesting antenna. It was shown that the coupling between the energy harvesting antenna and EM waves present in a given environment could be successfully simulated. This allows a designer to optimize e.g. the antenna's layout and position along its PCB.

Future work will cover the following directions: combining the aforementioned algorithm with a time-domain circuit simulator in order to calculate the total usable energy, taking into account typical modulation schemes as well as combining the proposed methodology with a ray-tracing algorithm in order to model a specific indoor electromagnetic environment.

6. References

1 Cook, D., Das, S.: 'Smart environments: Technology, protocols and applications', (John Wiley & Sons, Inc., 2004, 1st. edn.), pp. 1–18

2 Vullers, R., Schaijk, R., Visser, H., *et al.*: 'Energy Harvesting for Autonomous Wireless Sensor Networks', IEEE Solid-State Circuits Mag., 2010, 2, pp. 29–38

3 Beeby, S., White, N.: 'Energy harvesting for autonomous systems', (Artech House, 2010, 1st edn)

4 Pinuela, M., Mitcheson, P., Lucyszyn,S.: 'Ambient RF Energy Harvesting in Urban and Semi-Urban Environments', IEEE Trans. Microw. Theory Tech., 2013, 61, pp. 2715–2726

5 Dondi, D., Napoletano, G., Bertacchini,A., *et al.*: 'A WSN system powered by vibrations to improve safety of machinery with trailer', IEEE Sensors, Taipei, Republic of China, 2012, pp. 1–4

6 Yongtai,H., Lihui,L., Yanqiu,L.: 'Design of solar photovoltaic micro-power supply for application of wireless sensor nodes in complex illumination environments', IET Wirel. Sens. Syst., 2012, 2, pp. 16-21

7 Lu, X., Yang, S.-H.: 'Thermal energy harvesting for WSNs', IEEE International Conference on Systems Man and Cybernetics,Istanbul, Turkey, 2010, pp.3045–3052

8 Xie, Y., Wang, S., Lin, L., *et al.*: 'Rotary triboelectric nanogenerator based on a hybridized mechanism for harvesting wind energy', ACS Nano,2013,7,pp. 7119–25

9 Nikolov, D. , Manolov, E. , Hristov,M., *et al.*.: 'Architecture of Energy Harvesting Devices', Annu. J. Electron., 2010, 4, pp. 54–58

10 Chen, W., Wassell,I.: 'Energy-efficient signal acquisition in wireless sensor networks: a compressive sensing framework', IET Wirel. Sens. Syst., 2012, 2, pp. 1–8

11 Chuang, P.-J., Lin, C.-S.: 'Energy-efficient two-hop extension protocol for wireless body area networks', IET Wirel. Sens. Syst., 2013, 3, pp. 37–56

12 Kansal, A., Hsu, J., Zahedi,S., Srivastava, M.:'Power management in energy harvesting sensor networks', ACM Trans. Embed. Comput. Syst., 2007, 6, pp. 32–es

13 Cammarano, A., Petrioli,C., Spenza,D.: 'Pro-Energy: A novel energy prediction model for solar and wind energy-harvesting wireless sensor networks', IEEE 9th International Conference on Mobile Ad-Hoc and Sensor Systems,Las Vegas, Nevada, USA, 2012, pp. 75–83

14 Moser, C., Brunelli, D., Thiele, L., Benini, L.: 'Lazy scheduling for energy harvesting sensor nodes', in Kleinjohann, B., *et.al.*(6): 'From Model-Driven Design to Resource Management for Distributed Embedded Systems, (Springer US, 2010, 1st edn.), pp. 125–134

15 Liu, S., Wu, Q., Qiu, Q.: 'Accurate modeling and prediction of energy availability in energy harvesting real-time embedded systems', International Conference on Green Computing, 2010, pp. 469–476

16 Kurs, A., Karalis, A., Moffatt, R., *et al.*: 'Wireless power transfer via strongly coupled magnetic resonances.', Science, 2007, 317, pp. 83–86

17 Sun,Q., Patil,S., Stoute,S., Sun,N.-X., Lehman,B.: 'Optimum design of magnetic inductive energy harvester and its AC-DC converter', 2012 IEEE Energy Convers. Congr. Expo., 2012, pp. 394–400

18 Zhao, W., Choi, K., Bauman, S., *et al.*: 'A Radio-Frequency Energy Harvesting Scheme for Use in Low-Power Ad Hoc Distributed Networks', IEEE Trans. Circuits Syst. II Express Briefs, 2012, 59, pp. 573–577

19 Olgun, U., Chen, C.-C., Volakis, J. L.: 'Design of an efficient ambient WiFi energy harvesting system', IET Microwaves, Antennas Propag., 2012, 6, pp. 1200

20 Tucker, C.A., Warwick, K., Holderbaum, W.: 'Efficient wireless power delivery for biomedical implants', IET Wirel. Sens. Syst., 2012, 2, pp. 176

21 'Wireless Power Solutions|Powercast Corp.', http://www.powercastco.com/, accessed May 2013

22 Vullers, R., van Schaijk, R., Gyselinckx, B., Van Hoof, C.: 'Is there a sweet spot for energy harvesting?', Device Res. Conf., University Park, PA, USA 2009, pp. 7–8

23 Sakamoto, T., Ushijima, Y., Nishiyama, E., Aikawa, M., Toyoda, I.: '5.8-GHz Series/Parallel Connected Rectenna Array Using Expandable Differential Rectenna Units', IEEE Trans. Antennas Propag., 2013, 61, pp. 4872–4875

24 Hagerty, J.A., Helmbrecht,F. B., McCalpin, W.H., *et al.*: 'Recycling ambient microwave energy with broad-band rectenna arrays', IEEE Trans. Microw. Theory Tech., 2004, 52, pp. 1014–1024

25 Nintanavongsa, P., Muncuk, U.: 'Design Optimization and Implementation for RF Energy Harvesting Circuits', Top. Circuits, 2012, 2, pp. 24–33

26 Shams,R., Sadeghi, P.: 'On optimization of finite-difference time-domain (FDTD) computation on heterogeneous and GPU clusters', J. Parallel Distrib. Comput., 2011, 71, pp. 584–593

27 Keller, J.B.: 'Geometrical Theory of Diffraction', J. Opt. Soc. Am., 1962, 52, pp. 116

28 Kragalott, M., Kluskens, M. S., Zolnick, D.A., *et al.*.: 'A Toolset Independent Hybrid Method for Calculating Antenna Coupling', IEEE Trans. Antennas Propag., 2011, 59, pp. 443–451

29 Li, J.L.: 'Efficient Current-Based Hybrid Analysis of Wire Antennas Mounted on a Large Realistic Aircraft', IEEE Trans. Antennas Propag., 2010, 58, pp. 2666–2672

30 Vanhee, F., Pissoort, D., Catrysse, J., *et al.*.: 'Efficient Reciprocity-Based Algorithm to Predict Worst Case Induced Disturbances on Multiconductor Transmission Lines due to Incoming Plane Wavesloadlo', IEEE Trans. Electromagn. Compat., 2013, 55, pp. 208–216

31 Diallo, A., Luxey, C., Le Thuc, P., *et al.*: 'Diversity Performance of Multiantenna Systems for UMTS Cellular Phones in Different Propagation Environments', Int. J. Antennas Propag., 2008, 2008, pp. 1–10

32 Stutzman, W. L., Thiele, G. A.: 'Antenna theory and design', (J. Wiley, 1998)

33 Taga, T.: 'Analysis for mean effective gain of mobile antennas in land mobile radio environments', IEEE Trans. Veh. Technol., 1990, 39, pp. 117–131

34 Magdowski, M., Tkachenko, S.V., Vick, R.: 'Coupling of Stochastic Electromagnetic Fields to a Transmission Line in a Reverberation Chamber', IEEE Trans. Electromagn. Compat., 2011, 53, pp. 308–317

35 Weisstein, E.W.: 'Sphere Point Picking -- from Wolfram MathWorld'. Wolfram Research, Inc.

36 Hill, D.A.: 'Plane wave integral representation for fields in reverberation chambers', IEEE Trans. Electromagn. Compat., 1998, 40, pp. 209–217

37 Hill, D.A.: 'Electromagnetic Fields in Cavities', (John Wiley & Sons, Inc., 2009), pp. 280

38 'EMPro 3D EM Simulation Software|Agilent' http://www.home.agilent.com/en/pc-1297143/empro-3d-em-simulation-software?&cc=BE&lc=dut, accessed May 2013

39 Hill, D.A.: 'Electromagnetic theory of reverberation chambers', (NIST, 1998)